

Search for Dark Matter Produced in Association with a Higgs Boson Decaying to $b\bar{b}$ at $\sqrt{s} = 13$ TeV with the ATLAS Detector

Rainer Röhrig* on behalf of the ATLAS Collaboration

Max Planck Institute for Physics (Werner Heisenberg Institute), Munich

E-mail: rainer.roehrig@cern.ch

The existence of Dark Matter is inferred from several astrophysical and cosmological observations. Several extensions of the Standard Model accommodating the present theoretical and experimental Dark Matter constraints predict associated production of Dark Matter particles with the Standard Model Higgs boson. A search for such models is presented for the final state with large missing momentum and b -jets from the Higgs boson decay. The results are based on 36.1 fb^{-1} of pp collision data at a center-of-mass energy of 13 TeV recorded by the ATLAS detector at the Large Hadron Collider. An optimized event selection together with an improved Higgs boson identification in boosted topologies leads to a significant improvement in sensitivity compared to previous searches. The observed data are in good agreement with the Standard Model predictions. Thus, limits are placed on the cross-section for Dark Matter particle production in association with a Higgs boson, assuming a simplified theory model with two Higgs doublets and a heavy vector mediator. In addition, stringent model-independent limits are placed at the detector level on the production cross-section of processes beyond the Standard Model. These can be reinterpreted in the context of a wider range of theoretical models with the same event signature.

*EPS-HEP 2017, European Physical Society conference on High Energy Physics
5-12 July 2017
Venice, Italy*

*Speaker.

1. Introduction

A compelling candidate for Dark Matter (DM) is a stable electrically neutral particle χ whose non-gravitational interactions with Standard Model (SM) particles are weak. If the mass of such a particle is at the scale of electroweak symmetry breaking, the particle would accommodate the observed DM relic density and could be produced at the Large Hadron Collider (LHC). Most collider-based searches for DM rely on the signature of missing transverse momentum E_T^{miss} from DM particles recoiling against SM particle (e. g. gluon, photon, or a W or Z boson) radiated off the initial state. The discovery of the Higgs boson h opens a new opportunity through the $h + E_T^{\text{miss}}$ signature [1, 2, 3]. Since Higgs boson radiation off the initial state is Yukawa-suppressed, the $h + E_T^{\text{miss}}$ process represents a direct probe of the hard interaction involving the Higgs boson and DM particles. This poster presents a search for DM produced in association with a Higgs boson decaying into a pair of b -quarks ($h \rightarrow b\bar{b}$). The results are based on 36.1 fb^{-1} of pp collisions data at center-of-mass energy of 13 TeV recorded by the ATLAS detector [4] at the LHC. More details can be found in Ref. [5].

2. Interpretation

A Type-II two-Higgs-doublet model (2HDM) with an additional $U(1)_{Z'}$ gauge symmetry yielding an additional massive Z' boson provides an $h + E_T^{\text{miss}}$ signature [3] and is used for the interpretation of the observed data. In this simplified model containing five physical Higgs bosons, the $h + E_T^{\text{miss}}$ signature is produced via Z' mediator decays into two neutral Higgs bosons, the Standard-Model-like h and the pseudoscalar boson A . The h boson decays into b -quark pairs while the A boson decays into DM particles, $A \rightarrow \chi\bar{\chi}$. The Z' -2HDM model is defined by the following free parameters: the ratio $\tan\beta$ of the vacuum expectation values of the two Higgs fields coupling to the up-type and down-type quarks, the Z' gauge coupling $g_{Z'}$, and the masses $m_{Z'}$, m_A , and m_χ . The limits are set on the parameter plane spanned by the masses m_A and $m_{Z'}$, for fixed values of other three parameters. The results are also expressed in terms of limits on the production cross-section for non-SM $h + E_T^{\text{miss}}$ events without additional model assumptions, allowing for reinterpretation in the context of a wider range of theoretical models.

3. Event Selection

Events are selected by an E_T^{miss} trigger based on calorimeter information with a threshold of 110 GeV for most of the data taking period. Events are required to have at least one pp collision vertex reconstructed from at least two inner detector (ID) tracks. In order to apply a veto on electrons and muons in the final state, the reconstruction of those is performed. Identified muons must satisfy the loose quality criteria and have $|\eta| < 2.7$. Electrons are reconstructed by matching an ID track to a cluster of energy in the calorimeter and must satisfy the loose operating point and be within $|\eta| < 2.47$. Muon and electron candidates must have $p_T > 7 \text{ GeV}$ and are required to be isolated. Jets reconstructed with the anti- k_t algorithm are used to identify the products of the $h \rightarrow b\bar{b}$ decay. For small to moderate h momenta, the two h boson decay products can be resolved using jets with a radius parameter $R = 0.4$ (small- R jets or j). The central small- R jets

(with $|\eta| < 2.5$) must satisfy $p_T > 20$ GeV while the forward ones (with $2.5 < |\eta| < 4.5$) must have $p_T > 30$ GeV. The decay products of high-momenta h bosons become collimated and are reconstructed as a single jet with $R = 1.0$ (large- R or J). These jets are trimmed to reduce the effects of pileup and the underlying event. Furthermore, large- R jets must fulfill $p_T > 200$ GeV and $|\eta| < 2.0$. The mass of large- R jets is obtained by combining the tracking and calorimeter information. Multivariate b -tagging algorithms are used to identify jets containing b -hadrons and are applied on small- R jets or on the two leading track-based jets with highest p_T within a large- R jet. Track-based jets are reconstructed from ID tracks matched to the primary vertex using the anti- k_r algorithm with $R = 0.2$, and must fulfill $p_T > 10$ GeV and $|\eta| < 2.5$. The missing transverse momentum is calculated as the negative of the vector sum of the transverse momenta of e , μ , and jet candidates in the event, while p_T^{miss} uses only the tracks of the inner detector.

The signal is characterized by high E_T^{miss} ($E_T^{\text{miss}} > 150$ GeV) and jets yielding the mass of the h boson candidate which is compatible with the observed Higgs boson mass of around 125 GeV. No additional e or μ are allowed in the final state. The dominant background processes from $Z(\nu\nu) + \text{jets}$, $W + \text{jets}$, and $t\bar{t}$ production contribute respectively 30–60%, 10–25%, and 15–50% of the total background, depending on the size of E_T^{miss} and the b -tag multiplicity. The contributions of the $Z + \text{jets}$, $W + \text{jets}$ and $t\bar{t}$ are constrained using two control regions (CR): the single-muon control region is designed to constrain the $t\bar{t}$ and $W + \text{jets}$ backgrounds, while the two-lepton control region constrains the $Z + \text{jets}$ background contribution.

The multijet background contributes due to mismeasured jet momenta. To suppress it, additional selections are required: $\min \left[\Delta\phi \left(\vec{E}_T^{\text{miss}}, \vec{p}_T^j \right) \right] > \pi/9$ for the three highest- p_T (leading) small- R jets, $\Delta\phi \left(\vec{E}_T^{\text{miss}}, \vec{p}_T^{\text{miss}} \right) < \pi/2$, and $p_T^{\text{miss}} > 30$ GeV for events with fewer than two central b -tagged small- R jets.

In the *resolved* topology regime, defined by requiring $E_T^{\text{miss}} < 500$ GeV, the h boson candidate is reconstructed from two leading b -tagged central small- R jets, or, if only one b -tag is present in the event, from the b -tagged central small- R jet and the leading non- b -tagged central small- R jet. At least one of the jets comprising the h boson candidate must satisfy $p_T > 45$ GeV. The azimuthal separation $\Delta\phi$ between the h boson candidate and \vec{E}_T^{miss} of more than $2\pi/3$ is required. To improve the trigger efficiency modeling, events are retained only if the scalar sum H_T of the p_T of the two (three) leading jets fulfills $H_{T,2j} > 120$ GeV ($H_{T,3j} > 150$ GeV) if two (more than two) central jets are present. Events with a hadronic τ -lepton candidate, identified either by an algorithm based on a boosted decision tree or as small- R jet containing one to four tracks within the jet core and $\Delta\phi \left(\vec{E}_T^{\text{miss}}, \vec{p}_T^j \right) < \pi/8$, are rejected to reduce the $t\bar{t}$ background, which can enter the SR if at least one top quark decays as $t \rightarrow Wb \rightarrow \tau\nu b$. This background is further reduced by removing events with more than two b -tagged central jets. Since most of the hadronic activity in a signal event is expected from the $h \rightarrow b\bar{b}$ decay, the scalar sum of the p_T of the two jets forming the h boson candidate and, if present, the highest- p_T additional jet must be larger than $0.63 \times H_{T,\text{all jets}}$. Finally, $\Delta R \left(\vec{p}_h^{j_1}, \vec{p}_h^{j_2} \right) < 1.8$ is required for the two leading small- R jets forming the h boson candidate.

In the *merged* topology regime, defined by requiring $E_T^{\text{miss}} > 500$ GeV, the leading large- R jet represents the h boson candidate. Events containing τ -lepton candidates with $\Delta R \left(\vec{p}^\tau, \vec{p}^J \right) > 1.0$ are vetoed; no b -tagged central small- R jets with $\Delta R \left(\vec{p}^{j,b\text{-tag}}, \vec{p}^J \right) > 1.0$ are allowed in the event;

and the scalar sum of p_T of the small- R jets with $\Delta R(\vec{p}^J, \vec{p}^J) > 1.0$ is required to be smaller than 0.57 times that sum added to p_T^J .

The final discriminating variable is the mass of the Higgs boson candidate $m_{h,\text{reco}}$. In the resolved (merged) topology regime, this corresponds to the dijet invariant mass (mass of the leading large- R jet).

4. Background Estimation and Statistical Interpretation

The event selection in the single-muon CR is identical to the SR, except that exactly one isolated muon with $p_T^\mu > 27$ GeV is required, and that \vec{p}_T^μ is added to \vec{E}_T^{miss} to mimic the behavior of such events contaminating the SR when the muon is not detected.

Events in the two-lepton CR are collected using a single-electron or single-muon trigger, and selected by requiring one pair of isolated electrons or muons originating from a Z boson decay, one of which must have $p_T^\ell > 27$ GeV. In addition, a measure of the E_T^{miss} significance given by the ratio of the E_T^{miss} to the square root of the scalar sum of p_T of all leptons and small- R jets in the event must be less than $3.5 \text{ GeV}^{1/2}$. This requirement separates $Z(\ell\ell)$ +jets processes from $t\bar{t}$ production, as E_T^{miss} originates from finite detector resolution for the former and mainly from neutrinos for the latter. To mimic $Z \rightarrow \nu\nu$ decays in the SR, the \vec{E}_T^{miss} is redefined as the \vec{p}_T of the dilepton system. All other selection requirements are identical between the two-electron CR and the SR.

A fit to the $m_{h,\text{reco}}$ observable based on a binned likelihood approach is used to search for a signal. In order to interpret the observed data and search for DM signal, a fit of the expected to the observed $m_{h,\text{reco}}$ distribution is performed based on a binned likelihood approach. Experimental and theoretical systematic uncertainties are included in the likelihood function as nuisance parameters with Gaussian or log-normal constraints and profiled. Dominant sources of experimental systematic uncertainty arise from the limited number of simulated events, the calibration of the b -tagging efficiency and integrated luminosity, as well as the jet energy and mass scale and resolution uncertainties. Uncertainties associated with the τ -vetoes are found to be negligible. Dominant sources of theoretical systematic uncertainty originate from the modeling of the signal and background processes such as $t\bar{t}$, V +jets, Vh , diboson, and multijet production. This search is statistically limited for $E_T^{\text{miss}} > 300$ GeV.

To account for changes in the background composition and to benefit from a higher signal sensitivity with increasing E_T^{miss} and b -tag multiplicity, the data are split into categories that are fit simultaneously. Eight categories are defined for each of the SR and the two CRs: four ranges in E_T^{miss} with $[150, 200)$, $[200, 350)$, $[350, 500)$, and $[500, \infty)$ GeV, which are each split into two sub-regions with one and two b -tagged jets. In the one-muon CR, the electric charge of the μ is used to separate $t\bar{t}$ from W +jets since the former is characterized by an equal number of μ^+ and μ^- , while a prevalence of μ^+ is expected from the latter process. Only the total event yield is considered in the two-lepton CR due to limited amount of data. The normalizations of $t\bar{t}$, W +HF, and Z +HF processes are free parameters in the fit, where HF represents jets containing b - or c -quarks. In the SR, the normalization of Z +jets contribution is increased by about 50% after the fit, while $t\bar{t}$ is reduced by up to 30% at high E_T^{miss} . Subdominant backgrounds, including diboson, SM Wh and Zh , single top quark production are predicted directly from Monte Carlo simulation, while a data-driven method is used to estimate the multijet contribution.

Table 1: Observed (obs) and expected (exp) upper limits at 95% CL on $\sigma_{\text{vis},h(b\bar{b})+\text{DM}} = \sigma_{h+\text{DM}} \times \mathcal{B}(h \rightarrow b\bar{b}) \times \mathcal{A} \times \varepsilon$ of $h(b\bar{b}) + \text{DM}$ events [5]. Also shown are the acceptance \times efficiency ($\mathcal{A} \times \varepsilon$) probabilities to reconstruct and select an event in the same $E_{\text{T}}^{\text{miss}}$ bin as generated.

Range in $E_{\text{T}}^{\text{miss}}$ [GeV]	$\sigma_{\text{vis},h(b\bar{b})+\text{DM}}^{\text{obs}}$ [fb]	$\sigma_{\text{vis},h(b\bar{b})+\text{DM}}^{\text{exp}}$ [fb]	$\mathcal{A} \times \varepsilon$ [%]
[150, 200)	19.1	$18.3^{+7.2}_{-5.1}$	15
[200, 350)	13.1	$10.5^{+4.1}_{-2.9}$	35
[350, 500)	2.4	$1.7^{+0.7}_{-0.5}$	40
[500, ∞)	1.7	$1.8^{+0.7}_{-0.5}$	55

5. Results

The distributions of the $m_{h,\text{reco}}$ observable in the SR for events with two b -tags provide the highest signal sensitivity and are shown in the four $E_{\text{T}}^{\text{miss}}$ regions in Figure 1. No significant deviation from SM predictions is observed. The results are interpreted as exclusion limits at 95% confidence level (CL) on the production cross-section of $h + \text{DM}$ events $\sigma_{h+\text{DM}} \times \mathcal{B}(h \rightarrow b\bar{b})$ with the CL_S formalism using a profile likelihood ratio as test statistic. Exclusion contours in the $(m_{Z'}, m_A)$ parameter plane in the Z' -2HDM scenario are presented in Figure 2, excluding $m_{Z'}$ up to 2.6 TeV and m_A up to 0.6 TeV, substantially extending previous exclusion range.

Furthermore, upper limits are set on $\sigma_{\text{vis},h(b\bar{b})+\text{DM}} = \sigma_{h+\text{DM}} \times \mathcal{B}(h \rightarrow b\bar{b}) \times \mathcal{A} \times \varepsilon$ of $h(b\bar{b}) + \text{DM}$ events per $E_{\text{T}}^{\text{miss}}$ bin at detector level, after all SR selections except the requirements on $m_{h,\text{reco}}$ and b -tag multiplicity. The $\mathcal{A} \times \varepsilon$ term quantifies the probability for an event to be reconstructed in the same $E_{\text{T}}^{\text{miss}}$ bin as generated and to pass all $h(b\bar{b}) + \text{DM}$ selections, where \mathcal{A} represents the kinematic acceptance and ε accounts for the experimental efficiency. The results are shown in Table 1. To minimize the dependence on the $E_{\text{T}}^{\text{miss}}$ distribution of a potential $h+\text{DM}$ signal, the standard fit approach is modified to analyze one $E_{\text{T}}^{\text{miss}}$ range at a time in the SR.

The Z' -2HDM model is used to evaluate the dependence of the $\sigma_{\text{vis},h(b\bar{b})+\text{DM}}$ limits and of $\mathcal{A} \times \varepsilon$ on the event kinematics within a given $E_{\text{T}}^{\text{miss}}$ bin, assuming a generic back-to-back topology of the Higgs boson and $\vec{E}_{\text{T}}^{\text{miss}}$. A wide range of $(m_{Z'}, m_A)$ parameters that yield a sizable contribution in a given $E_{\text{T}}^{\text{miss}}$ bin is considered. Corresponding variations of 25% (70%) in the expected limits and of 50% (25%) in $\mathcal{A} \times \varepsilon$ are found in the resolved (merged) regime. Table 1 quotes the least stringent limit and the lowest $\mathcal{A} \times \varepsilon$ value in a given $E_{\text{T}}^{\text{miss}}$ bin after rounding. The limits are valid for $p_{\text{T},h} \lesssim 1.5$ TeV.

References

- [1] A. A. Petrov and W. Shepherd, *Searching for dark matter at LHC with Mono-Higgs production*, Phys. Lett. B **730** (2014) 178 [arXiv:1311.1511].
- [2] L. Carpenter et al., *Mono-Higgs-boson: A new collider probe of dark matter*, Phys. Rev. D **89** (2014) 075017 [arXiv:1312.2592].
- [3] A. Berlin, T. Lin and L. T. Wang, *Mono-Higgs Detection of Dark Matter at the LHC*, JHEP **1406** (2014) 078 [arXiv:1402.7074].

- [4] ATLAS Collaboration, *The ATLAS Experiment at the CERN Large Hadron Collider*, JINST **3** (2008) S08003.
- [5] ATLAS Collaboration, *Search for Dark Matter Produced in Association with a Higgs Boson Decaying to $b\bar{b}$ using 36 fb^{-1} of pp collisions at $\sqrt{s} = 13 \text{ TeV}$ with the ATLAS Detector*, To be submitted to PRL [arXiv:1707.01302].

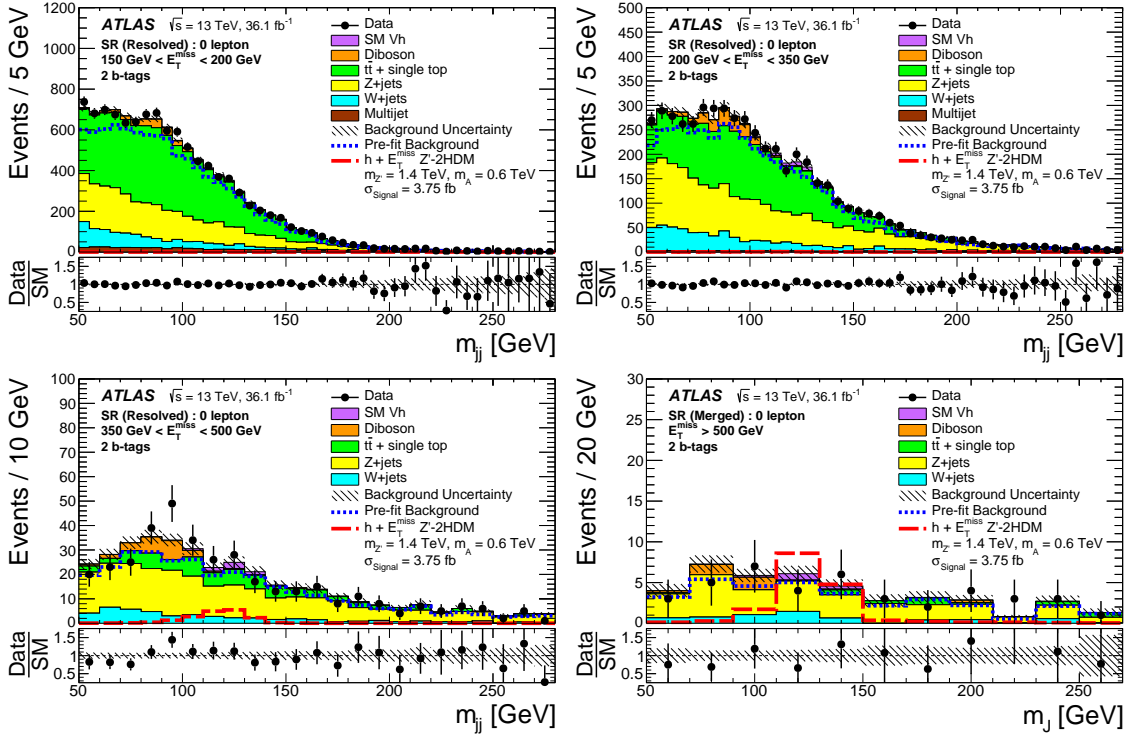


Figure 1: Distributions of the invariant mass of the Higgs boson candidates $m_{h, \text{reco}} = m_{jj}, m_J$ with two b -tags in the signal region for the four E_T^{miss} categories that are used as inputs to the fit [5]. The upper panels show a comparison of data to the SM expectation before (dashed lines) and after the fit (solid histograms) with no signal included. The lower panels display the ratio of data to SM expectations after the fit, with its systematic uncertainty considering correlations between individual contributions indicated by the hatched band. The expected signal from a representative Z' -2HDM model is also shown (long-dashed line).

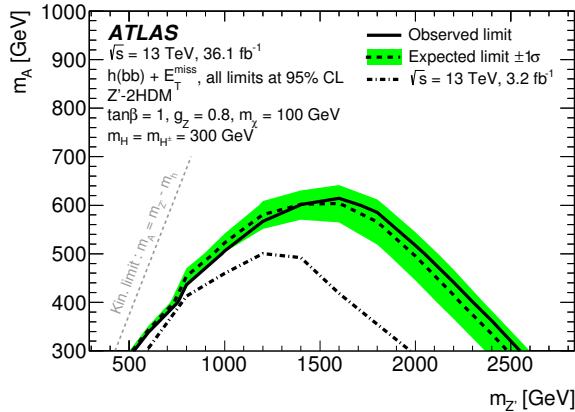


Figure 2: Exclusion contours for the Z' -2HDM scenario in the $(m_{Z'}, m_A)$ plane for $\tan\beta = 1$, $g_{Z'} = 0.8$, and $m_{\chi^0_1} = 100$ GeV [5]. The observed limits (solid line) are consistent with the expectation under the SM-only hypothesis (dashed line) within uncertainties (filled band). Observed limits from previous ATLAS results at $\sqrt{s} = 13$ TeV (dash-dotted line) are also shown.